Microfluidics and Nanofluidics (2020) 24:42
https://doi.org/10.1007/s10404-020-02346-2

RESEARCH PAPER

Preparation of mint oil microcapsules by microfluidics with high efficiency and controllability in release properties

Yuhan Du[1,2] · Liangji Mo[1,2] · Xiaoda Wang[1,2] · Hongxing Wang[1,2] · Xue-hui Ge[1,2] · Ting Qiu[1,2]

Received: 5 December 2019 / Accepted: 16 April 2020 / Published online: 6 May 2020

Abstract

Mint oil is a complex mixture of comparatively volatile and labile components, making it challenging to be efficiently encapsulated and retained in microcapsules using traditional approaches. Microencapsulation, by encapsulating the substance with certain shells, can effectively reduce the diffusion, evaporation and the reactions of the inside actives with the external environment. The microencapsulation of mint oil and other aromatic actives have been a prevailing method to improve the stability, prolong the storage time, and enhance the controllability of the actives. Monodisperse core–shell microcapsules based on double emulsions prepared by microfluidic technology with controllable structure, pH-responsive ability, and adjustable release properties are successfully developed. Different flow rates, glutaraldehyde concentration, solidification time and pH have been used to adjust the core sizes, the shell thickness, the crosslinking density and the shrinkage degree of the shell. By monitoring their mint oil sustained release ability through an ultraviolet spectrophotometer, appropriate conditions to form the mint oil microcapsules with high encapsulation efficiency and controllability in release properties are achieved, building the foundation for better mint oil storage, transportation, and their applications.

Keywords Microcapsule · Mint oil · Microfluidics · Chitosan · Controllable structure · pH responsive

1 Introduction

Mint oil is an aromatic vegetable oil extracted from the fresh stems and leaves of mint (Scartazzini et al. 2019). Its high medicinal value (Gao and Chen 2019) and versatile functions such as removing odor, increasing flavor, inhibiting bacterial growth, and preventing rot make it to be widely used in medicine, food (Salvia-Trujillo et al. 2015), fine chemicals and other fields. However, like most aromatic oils, mint oil is a complex mixture of comparatively volatile and labile components, such as β-pinene, limonene, methyl acetate, 3-octanol, and isomenthone (Beltagy and Beltagy 2019). Because of the existence of these volatile and labile components, mint oil is chemically unstable and susceptible to oxidation when exposed to oxygen, light, moisture and high temperature. It inevitably causes losses during storage and usage and limits their effective usage as additives in various products (Mishra et al. 2016).

To enhance physical and chemical properties or mask some undesirable aspects, a generic method is to encapsulate aromatic vegetable oil in inert shell to form microcapsules (Khalvandi et al. 2019). Microencapsulation, by encapsulating the substance with certain shells (Vian et al. 2016), can effectively reduce the diffusion, evaporation and the reactions of the inside actives with the external environment (Werner et al. 2018). Microcapsules can envelop a solid, liquid, or gaseous substance within another substance in a very small sealed capsule. The diameter of microcapsules is generally in the range of 1–1000 μm. Particles with a diameter of 1–1000 nm are called nanocapsules. Generally, microcapsules consist of a core material, which is referred to as the internal phase, and a shell. As a diffusion barrier, the shell is usually composed of various natural or synthetic

Electronic supplementary material The online version of this article (https://doi.org/10.1007/s10404-020-02346-2) contains supplementary material, which is available to authorized users.

✉ Xue-hui Ge
gexuehui@fzu.edu.cn

✉ Ting Qiu
tingqiu@fzu.edu.cn

[1] College of Chemical Engineering, Fuzhou University, Fuzhou 350116, China

[2] Engineering Research Center of Reactive Distillation, Fujian Province University, Fuzhou 350116, China

polymeric materials, encapsulating the core material and forming the external structure of the microcapsules (Abbaspourrad et al. 2013). The microcapsules can achieve the controlled release of the core material through diffusion control, dissolution control, degradation control, and stimulation control (Caballero Aguilar et al. 2019). The controlled release can be triggered by environmental temperature (Geng et al. 2018), pH (Mukhopadhyay et al. 2014), ionic concentration, and magnetic field (Ge et al. 2014). Microcapsules with controllability in release properties are used to deliver various compounds such as drugs (Chong et al. 2015), pesticides, fragrances and flavors, which can improve efficacy and safety (Yang et al. 2014). The microencapsulation of mint oil and other aromatic actives has been a prevailing method to improve the stability, prolong the storage time, and enhance the controllability of the actives for better storage, transportation, and application.

To the best of our knowledge, there are three major methods for preparing microcapsules: physical method, chemical method, and physical chemical method. The methods used to prepare microcapsules depend on the type and sensitivity of core materials, the type and properties of shell materials, the size of microcapsules, release mechanism, and the application of microcapsules (Martins et al. 2017). Commonly used microencapsulation techniques are (Bakry et al. 2016): spray drying, freeze drying, coacervation, solvent evaporation, multiphase emulsification, situ polymerization, centrifugal extrusion, fluidized-bed-coating, sharp hole-coagulation bath, and supercritical fluid technology, etc. The gelatin-gum Arabic coacervate microcapsules cross-linked with genipin encapsulate the mustard seed essential oil by complex coacervation technology (Peng et al. 2014), which maintains strong chemistry stability under different humidity and temperature and is potential for its application in food preservation. Mint oil microcapsules were prepared using Arabic gum alone and it blends with radiation or enzymatically depolymerized guar gum as shell materials by spray drying (Sarkar et al. 2012). The microcapsules were evaluated by principal component analysis and percent retention of mint oil. However, conventional encapsulation techniques have some common shortcomings, such as complex equipment operation, uncontrolled size, inefficient encapsulation, and low bioavailability (Ravanfar et al. 2018). These disadvantages would limit the efficient encapsulation, precise control, enhanced retention and wide applications of the core materials.

In recent years, a new method of microfluidic emulsification (Huang et al. 2017; Tregouet et al. 2019) has been proposed to produce monodisperse microcapsules (Wang et al. 2015). Microfluidic emulsification uses the fluid interfacial tensions to form emulsions (Ge et al. 2017). The size of the emulsion is determined by the flow rates of each phase and the size and structure of the microchannel (Wu and Gong 2013). Microfluidic emulsification makes monodisperse emulsions and microcapsules to be prepared simply and advances the research and application of microencapsulation in fine chemistry and biomedicine (Li et al. 2018; Su et al. 2016). The stable fragrance microcapsule is primarily prepared from bulk emulsification within polymer microcapsule via microfluidic emulsification (Lee et al. 2016) and demonstrates that enhanced retention can be achieved by a polar polymeric shell and forming a hydrogel network. The monodisperse core–shell microcapsule with acid-triggered burst release properties based on the crosslinked chitosan membrane is made by microfluidic emulsification, which enables microcapsules to be promising stomach-specific drug carrier candidates for quick and complete release. Although the microcapsules with high encapsulation efficiency and bioavailability are prepared by microfluidic emulsification in recent work, their control in the shell structure and core release rate are often complex (Lei et al. 2019; Zhao et al. 2014). They often need an increase of shell number (Choi et al. 2016) and modification of shell materials (Xia and Pack 2015). These methods often involve changes in microchannel structure and re-selection of shell materials. Therefore, there is an unmet need for an easy control strategy that enables the production of monodisperse microcapsules with controllable shell structure as well as the sustained release ability of core materials.

In this paper, we use flow focusing microchannel to prepare monodisperse mint oil/chitosan microcapsules. Based on the Schiff base reaction between chitosan and glutaraldehyde, the chitosan could form a stable shell with enough mechanical strength and pH-responsive ability. Different flow rates, glutaraldehyde concentration, solidification time and pH have been used to adjust the core sizes, the shell thickness, the crosslinking density and the shrinkage degree of the shell. By testing the sustained release rates of the mint oil microcapsules in air at room temperature, the appropriate conditions to form the mint oil microcapsules with high encapsulation efficiency and controllability in release property are achieved, building the foundation for better mint oil storage, transportation, and their applications.

2 Experimental

2.1 Materials

Mint oil was provided by Hubei Yongkuo Technology Co., Ltd. Chitosan (Viscosity 100–200 mPa·s, degree of deacetylation > 95%), glutaraldehyde (50% in H_2O), octane (96%), poly(ethylene glycol)-block-poly(propylene glycol)-block-poly(ethylene glycol) (PF-127, average Mn ~ 12,600), *n*-octanol and Span 80 was purchased from Shanghai Aladdin Bio-Chem Technology Co., Ltd. Acetic acid was

obtained from Xilong Chemical Co., Ltd., Guangdong. Ethanol was purchased from Guangdong Guanghua Sci-Tech Co., Ltd. All other reagents were analytically pure and used without further purification. Distilled water was from a laboratory-specific ultra-pure water machine purchased from Sichuan Wottle Water Treatment Equipment Co., Ltd.

2.2 Microfluidic device

The flow focusing microchannel was fabricated by assembling the cylindrical capillaries into square capillary tubes on glass slides. Cylindrical capillaries with inner and outer diameters of 0.60 mm and 0.95 mm, respectively, were used to fabricate the devices. The square capillary tubes with 1.0 mm inner diameters were slightly larger than that of the outer diameter of the cylindrical capillaries to ensure the coaxiality. The tips of the cylindrical capillaries were pulled by a vertical programmable puller (PC-100, Narishige, Japan) to form the injection capillary for fluids injection and the collection capillary for fluids collection. After they were polished to final outer diameters of 150 μm and 500 μm using sandpaper, respectively, they were inserted into a square capillary from the opposite direction and coaxially aligned within the square capillary tubes.

2.3 Fabrication of mint oil/chitosan microcapsules

Mint oil/chitosan microcapsules were prepared by a two-step process based on flow focusing microchannel: generation and solidification of monodispersed multiphase emulsion. Mint oil was injected through the cylindrical injection capillary as inner fluid. The aqueous solution containing 2% chitosan, 1% PF127, and 2% acetic acid was injected through the interstices of the square and injection capillaries from the same side with the injection capillary as middle fluid. *N*-octanol containing 2% span80 was injected through the square capillary from the other side as the outer fluid. Each phase was separately pumped into the flow focusing microchannel through poly tetra fluoro ethylene tube attached to disposable syringes. We used syringe pumps (Harvard Apparatus) to adjust the flow rates of each phase to form multiphase emulsion and control the structure and size in a glass capillary microfluidic device, as shown in Fig. 1a. The formation process of multiphase emulsion within flow focusing microchannel was monitored by an inverted microscope equipped (ECLIPSE Ts2R, Nikon, Japan) with a high-speed camera (FASTCAM SA1.1, Photron, Japan). The obtained O/W/O multiphase emulsions were collected into a coagulation bath, which consists of octane containing different concentrations glutaraldehyde and 2% span80, by poly tetra fluoro ethylene tube. The sizes of multiphase emulsions

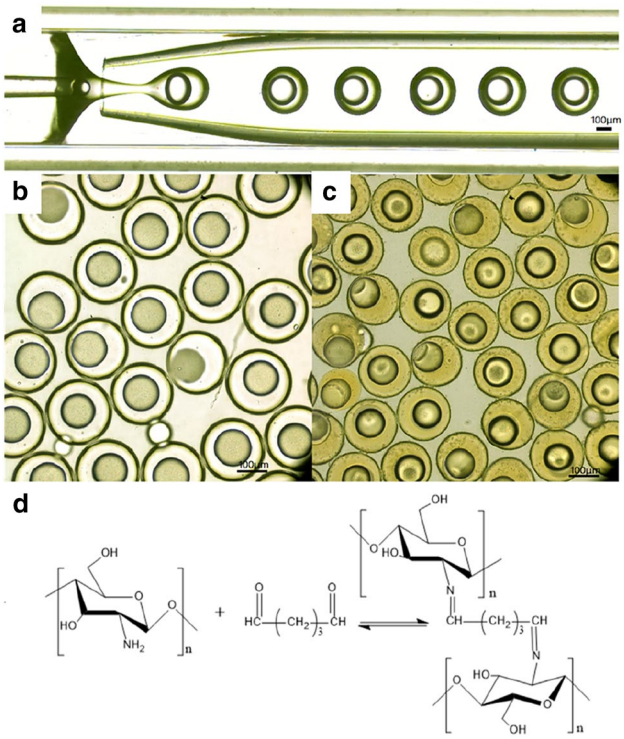

Fig. 1 Schematic illustration of the fabrication process of mint oil/chitosan microcapsules. **a** Glass capillary microfluidic device for preparing microcapsules. **b** Optical image of double emulsion. **c** Optical image of microcapsules solidified from double emulsions. Scale bar represents 100 μm. **d** Solidification mechanism: Schiff base reaction of glutaraldehyde and chitosan (Nematidil et al. 2019)

were measured by graphics software. Multiphase emulsions could be solidified to form mint oil/chitosan microcapsules by solvent extraction and chemical crosslinking based on Schiff base reaction, as shown in Fig. 1b and c. The shell of core–shell chitosan microcapsule was composed of glutaraldehyde-crosslinked chitosan hydrogel. It has been reported that chitosan can be crosslinked by glutaraldehyde with the formation of a Schiff base between the amino group of the chitosan and the aldehyde group of dialdehyde compounds in the neutral condition, as shown in Fig. 1d. The obtained microcapsules are washed using octane for several times.

2.4 FTIR characterization of chitosan and chitosan microcapsules

The chemical compositions of chitosan and chitosan microcapsules were confirmed via Fourier transform infrared spectrometry (FT-IR, Nicolet iS50, Thermo Fisher Scientific, USA) at 400–4000/cm with attenuated total refraction technique (ATR). Chitosan microcapsules for FT-IR measurement were prepared by the freeze drying method.

2.5 Morphological characterization of chitosan microcapsules

After microcapsules preparation, optical images are obtained using an inverted microscope equipped with a high-speed camera. The morphology of the microcapsules with different crosslinking density was observed using scanning electron microscopy (SEM, Helios G4 CX, Thermo Fisher Scientific, USA). The samples of microcapsules were dried by a freeze drying method for SEM observation.

2.6 Storage stability of the mint oil in chitosan microcapsules

To demonstrate the stability of mint oil encapsulated in the chitosan microcapsules, we monitored the remaining amount of mint oil over time in microcapsules using UV–vis spectroscopy (UV-2601, Beijing Beifen Ruili Analytical Instrument Co., Ltd.) at room temperature (approximately 25 °C). The microcapsules were rinsed at least three times with an excess volume of octane to remove the residual glutaraldehyde as well as the leaked mint oil before and during the rinsing procedure. Then, every fifty randomly selected microcapsules were transferred to different petri dishes at room temperature with time defined as $t = 0$ min. After certain different releasing time in various petri dishes, every group of microcapsules was dispersed in 2 mL deionized water to be sonicated for 10 min and then added to 3 mL ethanol s to be sonicated for 20 min to release all the remaining mint oil in the microcapsules. The content of residual mint oil was determined by the absorbance of the solution.

2.7 pH-responsive ability of chitosan microcapsules

The pH-responsive properties of the microcapsules were performed in a plastic petri dish with 0.2 mol/L phosphate buffer solutions (pH 1.5–5.5) at room temperature. Buffer solutions were prepared by NaH_2PO_4, Na_2HPO_4 and H_3PO_4 whose pH values were directly measured using an automatic potentiometric titrator (ZD-2, INESA Scientific Instrument Co., Ltd, Shanghai). Prior to tests, microcapsule samples had been saturated in deionized water for a few minutes. To change the ambient pH value in the microcapsule with different crosslinking density, excess buffer solution with a certain pH value was added into the petri dish rapidly at which time is defined as $t = 0$ min. The pH-responsive ability in size and morphology of microcapsules was monitored over time by an optical inverted microscope equipped with a high-speed camera.

3 Results and discussion

3.1 Morphology and size of microcapsules

The O/W/O double emulsions generated by flow focusing microchannel show clear core–shell structures and uniform sizes. The size of core and shell and the structure of the double emulsions could be adjusted by changing the flow rates of inner, middle and outer fluids. The core size and encapsulation frequency of double emulsions increased with the gradual increase of inner liquid flow rates from 1 to 19 μL/min when fixing the flow rate of middle and outer fluids, as shown in Fig. 2a. The core size decreased and the shell size increased at the same time with the gradual increase of middle liquid flow rates from 4 to 19 μL/min when fixing the flow rate of inner and outer fluids, as shown in Fig. 2b. And both the size of core and shell decreased simultaneously with the gradual increase of outer liquid flow rates from 50 to 650 μL/min when fixing the flow rate of inner and middle fluids, as shown in Fig. 2c.

Templated with the double emulsions, the core size, shell size and structure of the microcapsules could be adjusted by controlling the size and structure of the double emulsion correspondingly. Also, the sizes of the microcapsules decreased with the increase of the glutaraldehyde crosslinker concentration and the solidification time which result from shell solidification and the shell water extraction by octanol, as shown in Fig. 2d. Compared with the shell of double emulsions in octanol, the shell of microcapsules in glutaraldehyde solution changed from colorless and transparent to yellow, which also proved that double emulsion successfully solidified by Schiff base reaction. The size of microcapsules could be adjusted from 150 to 410 μm by adjusting the flow rate of each phase, solidification time and glutaraldehyde crosslinker concentration. This control strategy greatly enlarges the adjusting range of microcapsule size and provides a good foundation for the application of mint oil.

3.2 FTIR spectra of chitosan and chitosan microcapsules

The Fourier transform infrared analysis confirmed the crosslinking reaction between chitosan and glutaraldehyde. Compared with chitosan, there appeared a carbon–nitrogen double bond characteristic vibration at 1635/cm in curve of microcapsules, which verifies the successful occurrence of Schiff base reaction, as shown in Supporting Information Fig. S1. The mint oil/chitosan microcapsules were successfully prepared by microfluidic template double emulsion synthesis and Schiff base reaction.

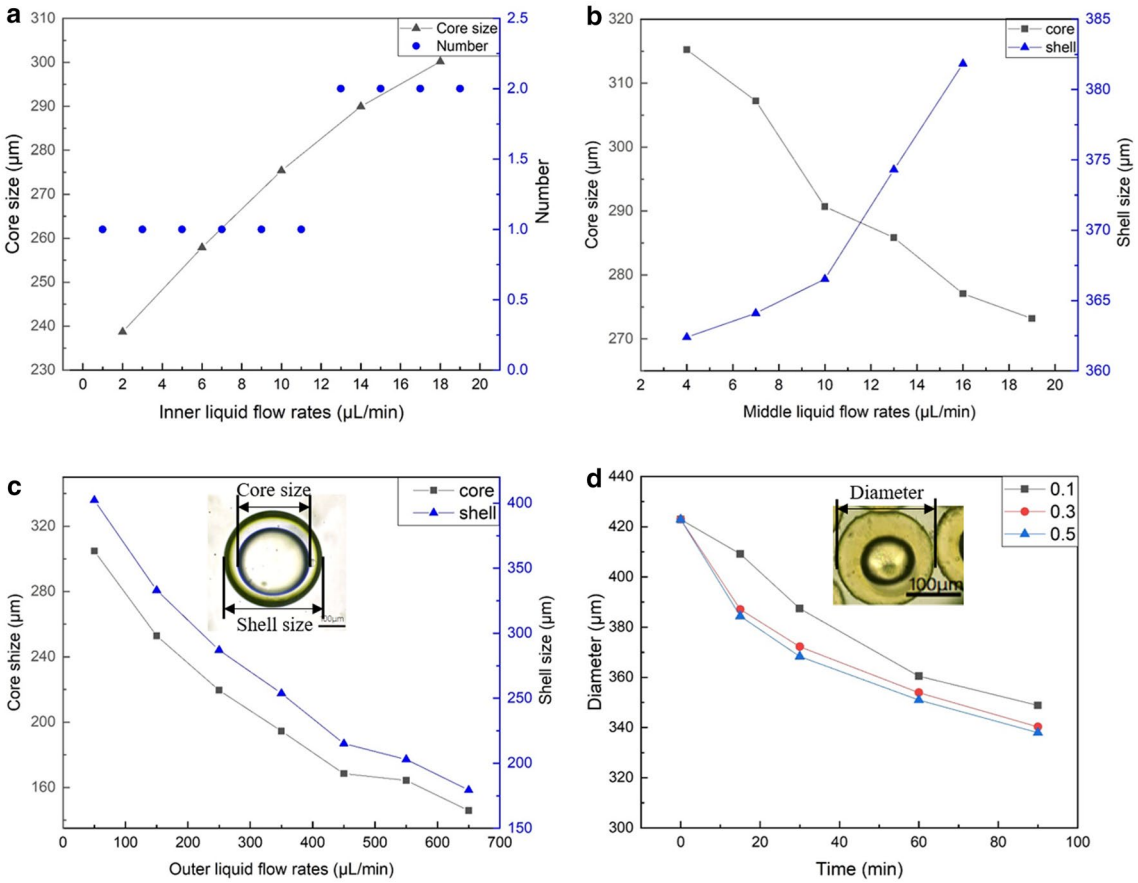

Fig. 2 Morphology and size regulation of microcapsules and double emulsions by **a** inner liquid flow rates, **b** middle liquid flow rates and **c** outer liquid flow rates, **d** solidification time and crosslinker concentration

3.3 Crosslinking density adjustment of microcapsules

When the double emulsions entered the coagulation bath, glutaraldehyde gradually diffused into the double emulsions and crosslinked with chitosan. Meanwhile, water in the shell gradually was extracted by *n*-octanol in the coagulation bath. Thus the relatively robust shell and the spherical shape of the microcapsules were achieved even when microcapsules are dried, which was directly confirmed by the SEM images. To further confirm the core–shell microstructure, the shells were broken by crushing the microcapsules using a sharp blade and the empty cores are directly visualized. The definition of the crosslinking density refers to the number of the crosslinking bonds per unit volume of the microcapsules. The higher crosslinking density represents the more crosslinking bonds per unit volume and the resultant higher crosslinking degree and more compact structure of the microcapsules. Through morphological characterization by the SEM, the crosslinking density would be qualitatively described. To achieve the controlled release of mint oil and regulate the release rate of mint oil, we need to prepare microcapsules with different crosslinking density, that is, microcapsules with different shell structures. By characterizing the sizes, the color and the structure of the microcapsule shells through optical images obtained by microscopy and SEM images, we found that the crosslinking density of microcapsules was mainly regulated by three methods: solidification time which was the residence time of templated double emulsion in coagulation bath; the shell size and the shell thickness of the templated double emulsions; crosslinker concentration which was glutaraldehyde concentration dissolved in coagulation bath.

3.3.1 Effect of solidification time

When the solidification time was 15 min, the shell of microcapsules turned light yellow with uniform size, high monodispersity and rough porous structure on the surface and inside, as shown in Fig. 3a. The shells at this time were composed of a reticulated skeleton structure formed by the initial crosslinking of chitosan and glutaraldehyde and a large amount of unextracted water existing in the polymer network space. After freeze drying, water was removed and

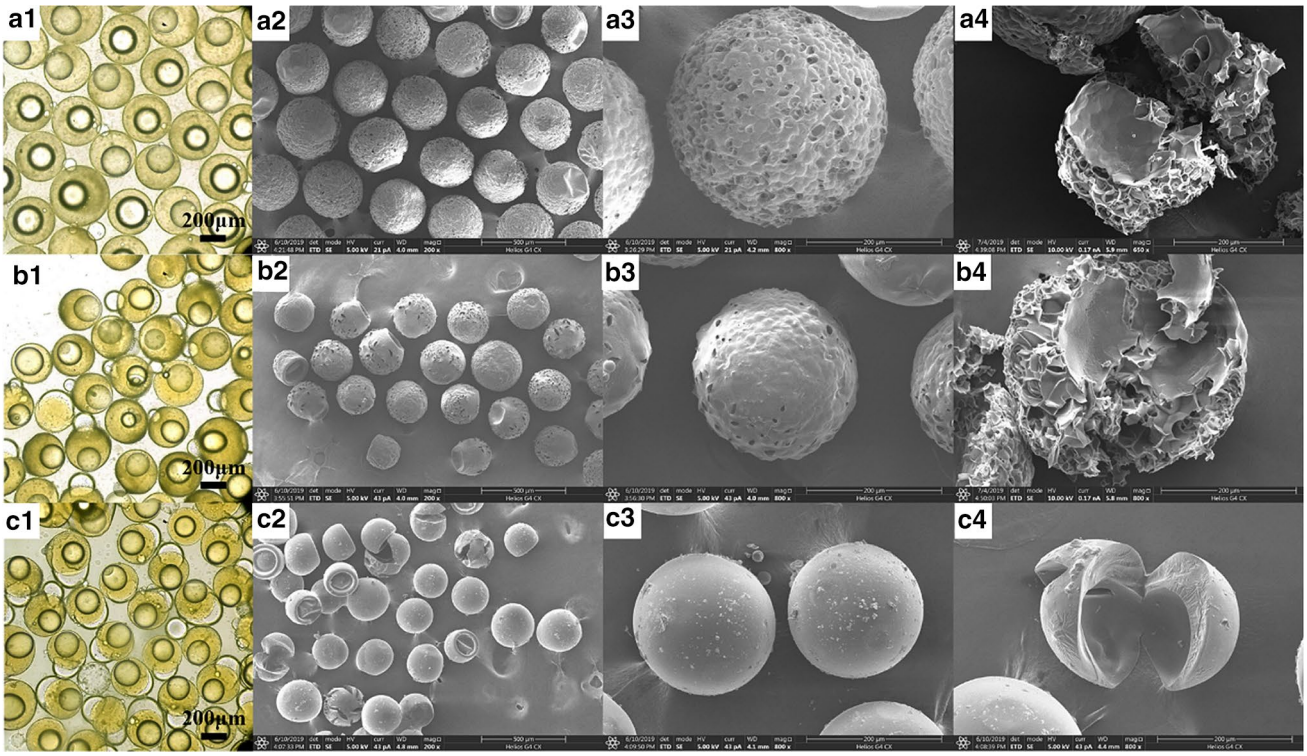

Fig. 3 Optical and SEM image of microcapsules with **a** 15 min, **b** 60 min and **c** 90 min solidification time. The inner, middle, and outer flow rates of the templated emulsions were 5 μL/min, 20 μL/min, and 100 μL/min, respectively. The glutaraldehyde concentration was 0.3 wt%

the rough porous structure was eventually formed. When the solidification time prolonged to 60 min, the shell color further deepened and the pores on the surface decreased gradually, while the internal structure remained rough porous, as shown in Fig. 3b. The water in the shell polymer network was extracted by *n*-octanol continuously, and the size of the microcapsule decreased gradually. When the curing time exceeded 90 min, the crosslinking and extraction process proceeded further, the shell color turned dark yellow and the shell eventually formed a whole smooth and compact structure, as shown in Fig. 3c. Glutaraldehyde entered the shell completely and crosslinked with chitosan, and the water in the microcapsules shell layer was completely extracted. The collapse of microcapsules shown in Fig. $3c_2$ was caused by the volatilization of the inner mint oil during freeze drying, which confirmed the hollow structure of the microcapsules. Thus, with the extension of the solidification time, the microcapsules had a darker yellow color, more compact shell structure, and smaller sizes, showing the higher crosslinking density.

3.3.2 Effect of templated double emulsion size

The sizes of the microcapsules which could be adjusted by the templated double emulsion sizes would also directly influence the crosslinking density by influencing the glutaraldehyde diffusion distances. Templated double emulsion with a 475 μm size and 243 μm shell thickness and a 437 μm size and 199 μm shell thickness, the microcapsules with the sizes of 309 μm and 205 μm had the rough porous structure on the surface and inside of shell after solidification, as shown in Fig. 4a and b. While keep reducing the templated emulsion size and shell thickness to 410 μm and 165 μm, the microcapsule with a 198 μm size eventually forms a whole smooth and compact shell structure, as shown in Fig. 4c. Glutaraldehyde could completely diffuse into the shell of microcapsules and crosslinked with chitosan within 90 min due to the shorter diffusion distance when the size and shell thickness were short enough. Thus, when fixing the glutaraldehyde concentration as 0.3 wt% and the solidification time as 90 min, we found that the microcapsules with bigger sizes and thicker shell have more rough shell structures while those with smaller sizes and thinner shell have more compact structures, showing the influence of the shell size and thickness in crosslinking density.

3.3.3 Effect of crosslinker concentration

It is easy to think that the crosslinking density would be influenced by the crosslinker concentration which is adjusted by the glutaraldehyde concentration in the solidification bath. With fixing the templated emulsion sizes and the

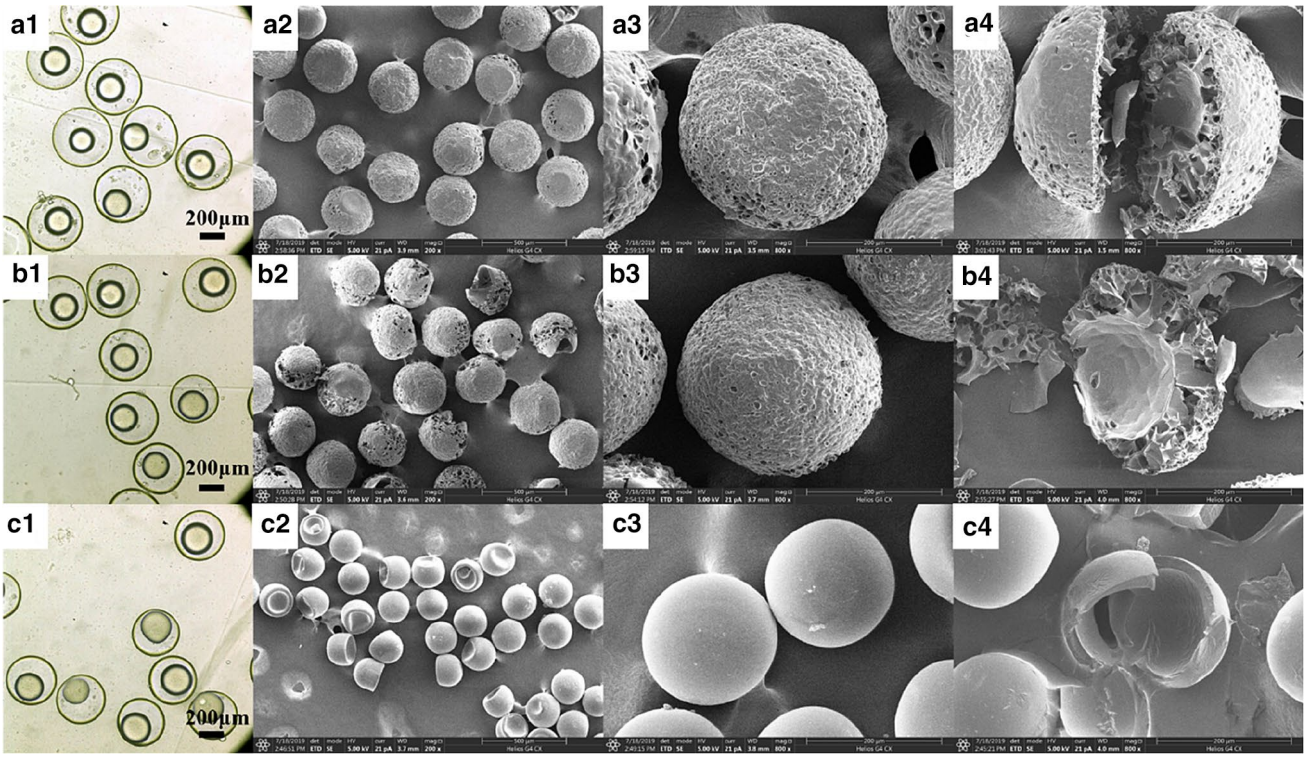

Fig. 4 Optical images of templated double emulsion with different size and shell thickness and SEM images of microcapsules. The glutaraldehyde concentration was 0.3 wt% and the solidification time was 90 min both in **a**–**c**. The inner flow rates and outer flow rates were 4 μL/min and 60 μL/min in **a**–**c** while the middle flow rates were **a** 20 μL/min, **b** 15 μL/min, **c** 10 μL/min, respectively

solidification time as 90 min, when the concentration of glutaraldehyde was only 0.1 wt%, the crosslinking density of microcapsules was not high enough to achieve the overall compact structure, as shown in Fig. 5a. When the concentration of glutaraldehyde was increased to 0.3 wt%, the surface and interior of microcapsules shell were smooth and compact, and a few microcapsules were not the overall compact structure, as shown in Fig. 5b. When the concentration of glutaraldehyde continued to increase to 0.5 wt%, all microcapsules were smooth and compact, as shown in Fig. 5c. Some microcapsules collapsed because the shell of microcapsules was thin at this solidification time and crosslinker concentration, and the strength of microcapsules during freeze drying was not enough, which verified the core–shell structure of microcapsules simultaneously. Thus the increasing glutaraldehyde concentration promoted the crosslinking between the chitosan and glutaraldehyde, resulting in more overall compact shell structure of the microcapsules.

To make a short summary of the above description, three typical structures of the microcapsules showing the different crosslinking density, such as integral porous structure, relatively compact surface while internal porous structure and integral compact structure, could be obtained by only controlling the solidification time, the size and thickness of the templated double emulsion and the crosslinking concentration. The microcapsules with these different structures could be prepared by only controlling any single condition, which greatly simplified the formation process and enhanced the control ability of the microcapsules, laying the foundation for the diversified and customized applications of the microcapsules.

3.4 Sustained release rates of mint oil in chitosan microcapsules in air at room temperature

Microcapsules with three typical shell structures, i.e. the integral porous structure, relatively compact surface while the internal porous structure and integral compact structure were used to test their different encapsulation effects for mint oil. Here, the microcapsule shell structures were adjusted by the solidification time. As the solidification time increased from 15 to 60 min, to 90 min, the structure of shell changed from integral porous to the compact surface while internal porous to the integral compact structure and the microcapsules sizes decreased with increasing solidification time, as shown in Fig. 3. And we defined residual ratio = residual concentration/initial concentration of the mint oil to compare the encapsulation effect of microcapsules with different structures. Higher residual ratio represented better mint oil encapsulation effect. The

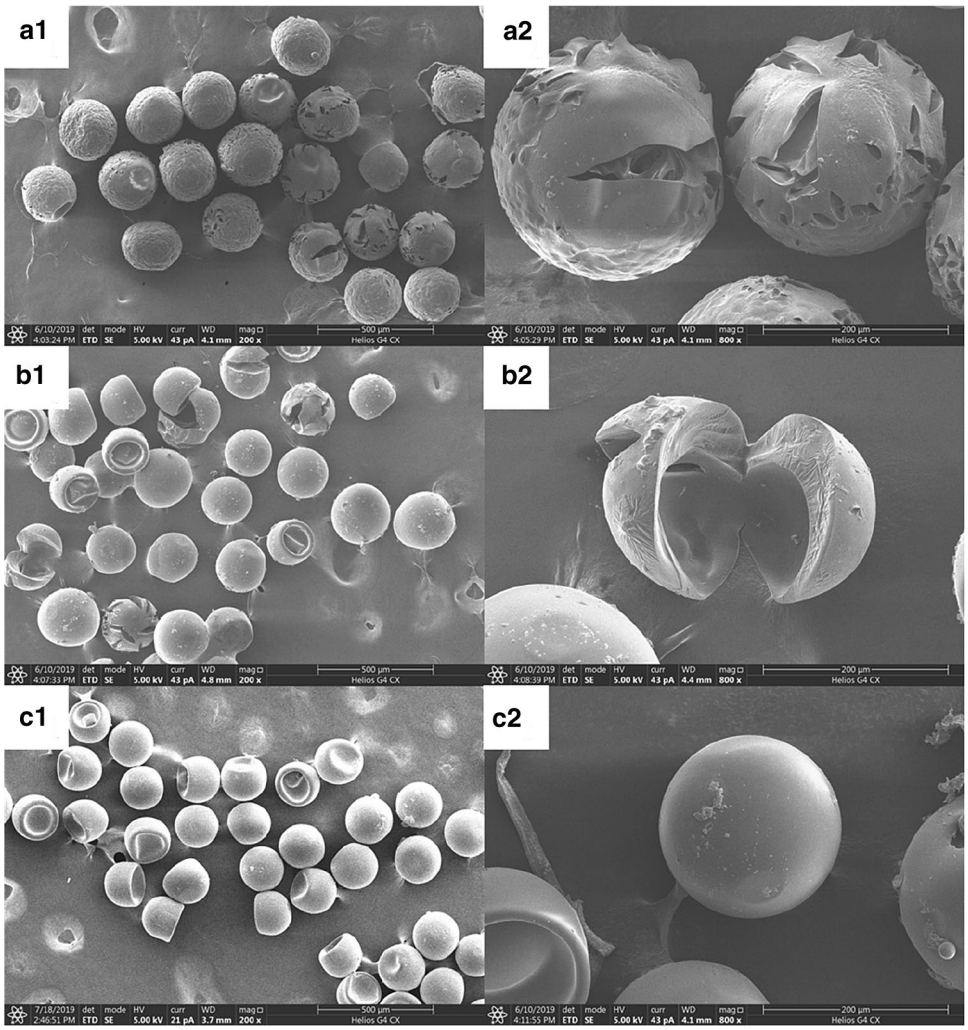

Fig. 5 SEM images of microcapsules with **a** 0.1 wt%, **b** 0.3 wt% and **c** 0.5 wt% crosslinking concentration. The inner, middle, and outer flow rates of the templated emulsions were 5 µL/min, 20 µL/min, and 100 µL/min, respectively. The solidification time was 90 min

residual concentration of mint oil in microcapsules in air at room temperature was monitored with time using UV–vis spectroscopy.

The standard curve regression equation of mint oil was obtained by linear regression of the concentration of mint oil with absorbance as follows:

$$y = 0.0242x + 0.1054.$$

The correlation coefficient $R = 0.9924$ showed that the absorption value of mint oil at 198 nm had a good linear relationship with the concentration, as shown in Fig. S2. For all tested microcapsules, the release rates were relatively fast before 240 min, and gradually slowed down after 240 min, and almost no longer released to the air after 1440 min, as shown in Fig. 6a. The concentration of mint oil in microcapsules with 15, 60 and 90 min solidification time decreased from $27*10^{-3}$ to $13*10^{-3}$ mg/mL, from $23*10^{-3}$ to $9*10^{-3}$ mg/mL and from $18*10^{-3}$ to $12*10^{-3}$ mg/mL respectively with the release time from 0 to 1440 min. The microcapsules with 90 min solidification time had the best encapsulation effect and the slowest release rate, followed by 15 min and 60 min, as shown in Fig. 6b. The microcapsules with overall smooth and compact shell structure solidified in 90 min could effectively prevent the mint oil diffusing from the inside of the microcapsules into the air, so the encapsulation effect was good and about 72% encapsulated mint oil remained at 1440 min when stored in air at room temperature. The porous structures in the interior shell and integral shells of the microcapsules with 60 min and 15 min solidification time resulted in their worse encapsulation effect than those with 90 min solidification time. About only 48% and 56% encapsulated mint oil in microcapsules remained at 1440 min in microcapsules solidified in 60 min and 15 min, respectively. It was noteworthy that the microcapsules with integral porous shell solidified in 15 min had better encapsulation effect than those with only interior pores and relatively compact shell surface structure solidified in 60 min. The reason might be related to the shell

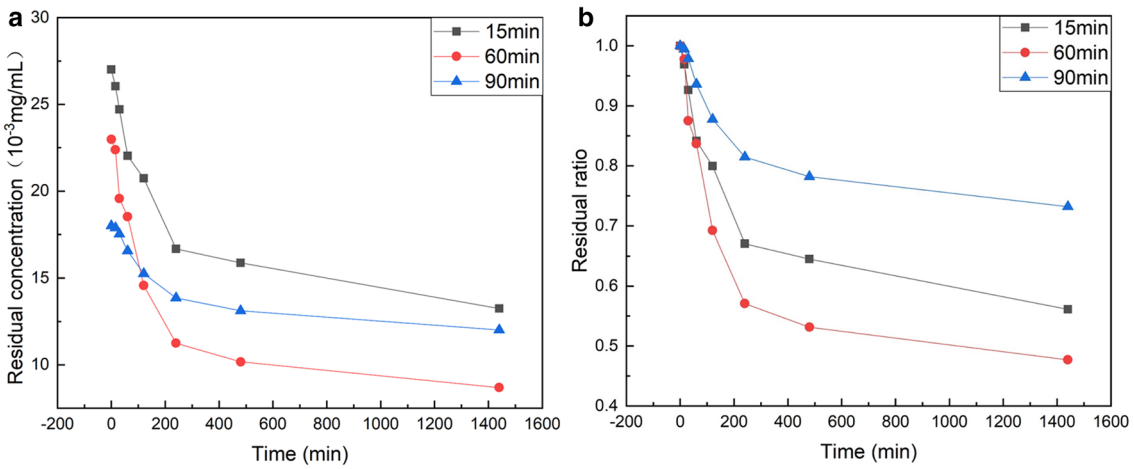

Fig. 6 **a** Residual concentration versus time with variation in the different solidification. **b** Residual ratio versus time with variation in the different solidification

thickness. The former microcapsules had the thicker shell and the diffusion distance of the mint oil from the inside of the microcapsules into the air was relatively long. The porous shell and the relatively thinner shell of the microcapsules solidified in 60 min resulted in the easier mint oil release, shorter diffusion distance from the inside of the microcapsules into the air and thus the unsatisfactory encapsulation effect.

For the microcapsules, the longer solidification time could result into the more compact structure with less existing water in the shell and result to the more hydrophobic property which might increase the mint oil retaining ability. Thus the longer solidification time and thicker microcapsule shell could prolong the retention time of the mint oil, representing a better encapsulation effect.

3.5 pH-responsive ability of chitosan microcapsules

Chitosan is a de-acetylated product of chitin and is one of the most abundant natural polymers in nature. Because it is a biocompatible, easily biodegradable and non-toxic polymer material, it is widely used in biology, medicine, cosmetics and other fields. The crosslinking of chitosan and glutaraldehyde could form pH sensitive hydrogels. So we want to find out how the pH would influence the swelling and contraction of chitosan hydrogels. To estimate the pH-responsive ability of chitosan microcapsules, the shrinkage processes of chitosan microcapsules in the pH range of 1.5–5.5 were studied systematically. Microcapsules were firstly immersed in a small amount of deionized water. Then, we introduced a sudden change to the pH value of their environmental solution by quickly adding a large amount of phosphate buffer solution with different pH values. The

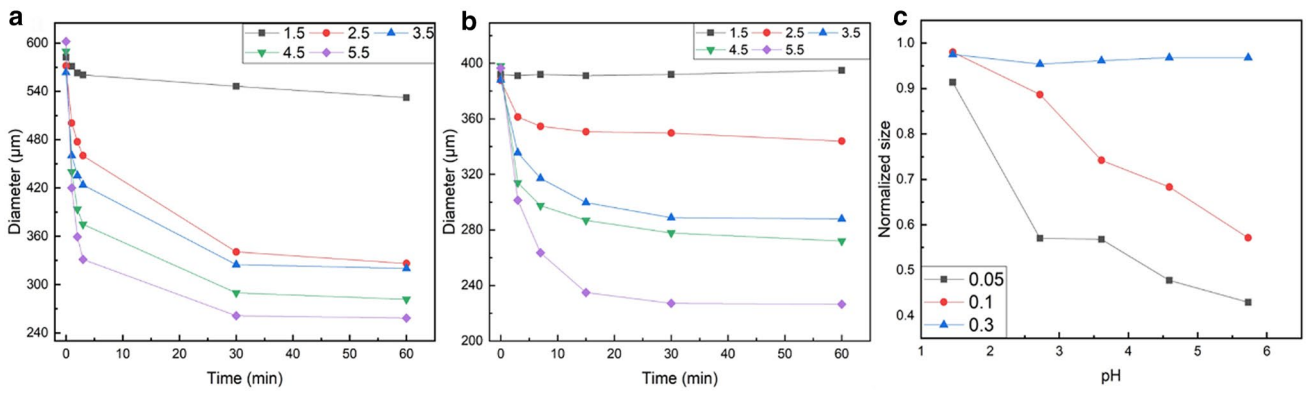

Fig. 7 pH-responsive ability of chitosan microcapsules with different crosslinking concentration and pH value. **a** 0.05 wt% crosslinking concentration, **b** 0.1 wt% crosslinking concentration. **c** Normalized size of microcapsules with different crosslinking concentration under different pH conditions

shrinkage of microcapsules with 0.05 wt% crosslinking concentration in different environmental pH values was shown in Fig. 7a. When the environmental pH value was 1.5, the size of the microcapsules decreased from 583 to 532 μm and the size decreased to 91% of the initial size. When the environmental pH value was 5.5, the size of the microcapsules was decreased from 602 to 258 μm and the size decreased to 43% of the initial size. The shrinkage of microcapsules with 0.1 wt% crosslinking concentration in different environmental pH values was shown in Fig. 7b. When the environmental pH value was 1.5, the size of the microcapsules has hardly changed. When the environmental pH value increased to 5.5, the size of the microcapsules was decreased from 397 to 226 μm and the size decreased to 57% of the initial size. To compare the shrinkage degree of the microcapsules with different crosslinking concentration under different pH conditions, we defined normalized size = size after shrinkage/initial size to express the result. The shrinkage of microcapsules increased with the decrease of crosslinking concentration and the increase of pH value in acidic conditions, as shown in Fig. 7c. When the glutaraldehyde concentration was 0.3 wt%, the size of microcapsules did not change significantly in an acidic environment. When the glutaraldehyde concentration decreased to 0.1 wt%, the sizes of microcapsules shrunk to 0.89, 0.74, 0.68 and 0.57 respectively with the pH value gradual increase from 2.5 to 5.5. When the glutaraldehyde concentration continued to decrease to 0.05 wt%, the shrinkage of microcapsules was more obvious under acidic conditions.

From the results, we found that the influence of pH is different when the solution acidity and microcapsule crosslinking degree (adjusted by the crosslinker concentration) are different. The higher the environmental pH value in acidic conditions is, the faster the acid-triggered shrinking of the microcapsule shell would be, as shown in Fig. 7a and b. And the lower crosslinking density (the lower glutaraldehyde concentration), the more significant shrinkage of the microcapsules under acidic conditions, as shown in Fig. 7c. The rapid shrinkage of chitosan hydrogels would result into the shell rupture and the total release of the mint oil (Showing in the supporting material Gif. S1). And the gradual shrinkage of the chitosan hydrogel would result into the higher crosslinking density and thicker shell of the microcapsules, which is resulted into better retain ability of the mint oil, which have been revealed in Sect. 3.4.

4 Conclusions

Here, we introduce the strategy of the combining solidification method of solvent extraction and chemical crosslinking to prepare monodispersed mint oil/chitosan microcapsules with high encapsulation efficiency, good spherical shape and stable shell with enough mechanical strength based on templated double emulsions formed with microfluidic technology. The size and encapsulation frequency of microcapsules can be conveniently controlled by flow rates of fluids. Different solidification time, sizes of templated double emulsions and crosslinking concentration have been used to adjust the microcapsules structures. Three typical microcapsule structures are formed and their encapsulation effects of the mint oil are tested. The microcapsules with overall smooth and compact shell structure could effectively prevent the mint oil diffusing and about 72% encapsulated mint oil remained after 24 h when stored in air at room temperature. Also, the pH-responsive ability of the chitosan microcapsules is researched. The shrinkage degree and speed of the shell could be adjusted by pH and crosslinking concentration. Thus the appropriate conditions to form the mint oil microcapsules with high encapsulation efficiency and controllability in release property are achieved, building the foundation for better mint oil or other aromatic oils storage, transportation and their applications.

Acknowledgements This work was supported by National Natural Science Foundation of China (Grant No. 21908026), Open Grant from The United State Key Laboratory of Chemical Engineering in Tsinghua University (No. SKL-ChE-18A04), and Fuzhou University Testing Fund of precious apparatus (2019T020 and 2019T021).

References

Abbaspourrad A, Carroll NJ, Kim SH, Weitz DA (2013) Polymer microcapsules with programmable active release. J Am Chem Soc 135:7744–7750. https://doi.org/10.1021/ja401960f

Bakry AM, Abbas S, Ali B, Majeed H, Abouelwafa MY, Mousa A, Liang L (2016) Microencapsulation of oils: a comprehensive review of benefits, techniques, and applications. Compr Rev Food Sci Food Saf 15:143–182. https://doi.org/10.1111/1541-4337.12179

Beltagy AM, Beltagy DM (2019) Quality control chemical composition and antioxidant activity of some marketed peppermint oil samples. Int J Pharm Sci Res 10:3865–3872. https://doi.org/10.13040/ijpsr.0975-8232.10(8).3865-72

Caballero Aguilar LM, Kapsa RM, O'Connell CD, McArthur SL, Stoddart PR, Moulton SE (2019) Controlled release from PCL-alginate microspheres via secondary encapsulation using GelMA/HAMA hydrogel scaffolds. Soft Matter 15:3779–3787. https://doi.org/10.1039/c8sm02575d

Choi CH et al (2016) Triple emulsion drops with an ultrathin water layer: high encapsulation efficiency and enhanced cargo retention in microcapsules. Adv Mater 28:3340–3344. https://doi.org/10.1002/adma.201505801

Chong D et al (2015) Advances in fabricating double-emulsion droplets and their biomedical applications. Microfluid Nanofluid 19:1071–1090. https://doi.org/10.1007/s10404-015-1635-8

Gao W, Chen Y (2019) Microencapsulation of solid cores to prepare double emulsion droplets by microfluidics. Int J Heat Mass Transf 135:158–163. https://doi.org/10.1016/j.ijheatmasstransfer.2019.01.136

Ge XH, Huang JP, Xu JH, Luo GS (2014) Controlled stimulation-burst targeted release by smart decentered core-shell microcapsules in

gravity and magnetic field. Lab Chip 14:4451–4454. https://doi.org/10.1039/c4lc00645c

Ge XH, Geng YH, Zhang QC, Shao M, Chen J, Luo GS, Xu JH (2017) Four reversible and reconfigurable structures for three-phase emulsions: extended morphologies and applications. Sci Rep 7:42738. https://doi.org/10.1038/srep42738

Geng YH, Ge XH, Zhang SB, Zhou YW, Wang ZQ, Chen J, Xu JH (2018) Microfluidic preparation of flexible micro-grippers with precise delivery function. Lab Chip 18:1838–1843. https://doi.org/10.1039/c8lc00293b

Huang H, Yu Y, Hu Y, He X, Berk Usta O, Yarmush ML (2017) Generation and manipulation of hydrogel microcapsules by droplet-based microfluidics for mammalian cell culture. Lab Chip 17:1913–1932. https://doi.org/10.1039/c7lc00262a

Khalvandi M, Amerian M, Pirdashti H, Keramati S, Hosseini J (2019) Essential oil of peppermint in symbiotic relationship with *Piriformosporaindica* and methyl jasmonate application under saline condition. Ind Crop Prod 127:195–202. https://doi.org/10.1016/j.indcrop.2018.10.072

Lee H, Choi CH, Abbaspourrad A, Wesner C, Caggioni M, Zhu T, Weitz DA (2016) Encapsulation and enhanced retention of fragrance in polymer microcapsules. ACS Appl Mater Interfaces 8:4007–4013. https://doi.org/10.1021/acsami.5b11351

Lei C et al (2019) Controlled reversible buckling of polydopamine spherical microcapsules: revealing the hidden rich phenomena of post-buckling of spherical polymeric shells. Soft Matter 15:6504–6517. https://doi.org/10.1039/c9sm00705a

Li W et al (2018) Microfluidic fabrication of microparticles for biomedical applications. Chem Soc Rev 47:5646–5683. https://doi.org/10.1039/c7cs00263g

Martins E, Poncelet D, Rodrigues RC, Renard D (2017) Oil encapsulation techniques using alginate as encapsulating agent: applications and drawbacks. J Microencapsul 34:754–771. https://doi.org/10.1080/02652048.2017.1403495

Mishra N et al (2016) Encapsulation of mentha oil in chitosan polymer matrix alleviates skin irritation. AAPS PharmSciTech 17:482–492. https://doi.org/10.1208/s12249-015-0378-x

Mukhopadhyay P, Sarkar K, Bhattacharya S, Bhattacharyya A, Mishra R, Kundu PP (2014) pH sensitive *N*-succinyl chitosan grafted polyacrylamide hydrogel for oral insulin delivery. Carbohydr Polym 112:627–637. https://doi.org/10.1016/j.carbpol.2014.06.045

Nematidil N, Sadeghi M, Nezami S, Sadeghi H (2019) Synthesis and characterization of Schiff-base based chitosan-*g*-glutaraldehyde/NaMMTNPs-APTES for removal Pb(2+) and Hg(2+) ions. Carbohydr Polym 222:114971. https://doi.org/10.1016/j.carbpol.2019.114971

Peng C, Zhao SQ, Zhang J, Huang GY, Chen LY, Zhao FY (2014) Chemical composition, antimicrobial property and microencapsulation of mustard (*Sinapisalba*) seed essential oil by complex coacervation. Food Chem 165:560–568. https://doi.org/10.1016/j.foodchem.2014.05.126

Ravanfar R, Comunian TA, Dando R, Abbaspourrad A (2018) Optimization of microcapsules shell structure to preserve labile compounds: a comparison between microfluidics and conventional homogenization method. Food Chem 241:460–467. https://doi.org/10.1016/j.foodchem.2017.09.023

Salvia-Trujillo L, Rojas-Graü A, Soliva-Fortuny R, Martín-Belloso O (2015) Physicochemical characterization and antimicrobial activity of food-grade emulsions and nanoemulsions incorporating essential oils. Food Hydrocoll 43:547–556. https://doi.org/10.1016/j.foodhyd.2014.07.012

Sarkar S, Gupta S, Variyar PS, Sharma A, Singhal RS (2012) Irradiation depolymerized guar gum as partial replacement of gum Arabic for microencapsulation of mint oil. Carbohydr Polym 90:1685–1694. https://doi.org/10.1016/j.carbpol.2012.07.051

Scartazzini L et al (2019) Gelatin edible coatings with mint essential oil (*Menthaarvensis*): film characterization and antifungal properties. J Food Sci Technol 56:4045–4056. https://doi.org/10.1007/s13197-019-03873-9

Su Y, Zhao H, Wu J, Xu J (2016) One-step fabrication of silica colloidosomes with in situ drug encapsulation. RSC Adv 6:112292–112299. https://doi.org/10.1039/c6ra19048k

Tregouet C, Salez T, Monteux C, Reyssat M (2019) Microfluidic probing of the complex interfacial rheology of multilayer capsules. Soft Matter 15:2782–2790. https://doi.org/10.1039/c8sm02507j

Vian A, Favrod V, Amstad E (2016) Reducing the shell thickness of double emulsions using microfluidics. Microfluid Nanofluid. https://doi.org/10.1007/s10404-016-1827-x

Wang Y, Jing Y, Hou H, Xu J, Wang Y (2015) Extraction of lanthanides by polysulfone microcapsules containing EHPNA. II Coaxial microfluidic method. J Rare Earths 33:765–775. https://doi.org/10.1016/s1002-0721(14)60483-x

Werner JG, Deveney BT, Nawar S, Weitz DA (2018) Dynamic microcapsules with rapid and reversible permeability switching. Adv Func Mater 28:1803385. https://doi.org/10.1002/adfm.201803385

Wu B, Gong HQ (2013) Formation of fully closed microcapsules as microsensors by microfluidic double emulsion. Microfluid Nanofluid 14:637–644. https://doi.org/10.1007/s10404-012-1083-7

Xia Y, Pack DW (2015) Uniform biodegradable microparticle systems for controlled release. Chem Eng Sci 125:129–143. https://doi.org/10.1016/j.ces.2014.06.049

Yang C et al (2014) Beta-cyclodextrin-based molecular-recognizable smart microcapsules for controlled release. J Mater Sci 49:6862–6871. https://doi.org/10.1007/s10853-014-8388-8

Zhao H, Xu JH, Wang T, Luo GS (2014) A novel microfluidic approach for preparing chitosan-silica core-shell hybrid microspheres with controlled structures and their catalytic performance. Lab Chip 14:1901–1906. https://doi.org/10.1039/c4lc00079j